

# MAGNETIZED DYNAMIC FRICTION FORCE IN THE STRONG-FIELD, SHORT-INTERACTION-TIME LIMIT\*

I.V. Pogorelov<sup>†</sup> and D.L. Bruhwiler, RadiaSoft LLC, Boulder, CO, USA

## Abstract

Relativistic magnetized electron cooling is one of the techniques explored for achieving the ion beam luminosity requirements of the presently designed electron-ion collider (EIC) facility at Brookhaven National Lab. Because the cooling system will have to operate in previously untested parameter regimes, accurate computation of magnetized dynamic friction is required at the design stage in order to obtain reliable estimates of the cooling time. At energies of interest to the EIC cooling system design, the beam-frame interaction time in the cooler becomes short compared to the plasma period, and some assumptions applicable to the physics of cooling at lower energies become invalid in this high-energy setting. We present and discuss the results of first-principles modeling the magnetized dynamic friction force in the strong-field, short-interaction-time regime, as well as a parametric longitudinal friction force model that we developed starting with a reduced ion-electron interaction potential. The model parameters are related in a simple way to the interaction time and the ion charge. We compare our simulation results to the predictions of previously developed theoretical models.

## REDUCED 1D ION-ELECTRON INTERACTION MODEL

We follow the general approach of Derbenev [1], wherein the total time-dependent E-field at the location of the ion  $\vec{E}(\vec{r}, \vec{v}, t)$  is viewed as comprised of three contributions: (i)  $\langle \vec{E}^0 \rangle(\vec{r}, t)$ , the Coulomb field from the bulk charge of the electron distribution, (ii)  $\langle \Delta \vec{E} \rangle(\vec{r}, \vec{v}, t)$ , the dynamic friction force, the occurrence of which is due specifically to the modulation of the electron phase space distribution caused by the presence of the ion, and (iii)  $\vec{E}^{fl}(\vec{r}, \vec{v}, t)$ , statistical fluctuations due to irregularity of the electron distribution at the microscopic scale:

$$\vec{E}(\vec{r}, \vec{v}, t) = \langle \vec{E}^0 \rangle(\vec{r}, t) + \langle \Delta \vec{E} \rangle(\vec{r}, \vec{v}, t) + \vec{E}^{fl}(\vec{r}, \vec{v}, t). \quad (1)$$

The friction force is then calculated along the ion trajectory:

$$\vec{F}(\vec{r}, \vec{v}, t) = -Ze \langle \Delta \vec{E} \rangle(\vec{r}, \vec{v}, t) \Big|_{\vec{r}=\vec{r}(t), \vec{v}=\vec{v}(t)}. \quad (2)$$

In practice, of interest is the dynamic friction force averaged over the time it takes the beams to traverse the cooler solenoid, which is what we compute in this paper. Furthermore, in this paper we limit discussion to the computation of the ensemble-averaged expectation value of the friction

force for the ion moving longitudinally (along the magnetic field lines). We assume a constant and uniform magnetic field in the solenoid.

By short interaction time we mean interaction time  $T_{int}$  short compared to the beam-frame plasma period  $T_{pl} = \sqrt{\pi/n_e r_e c^2}$ , where  $n_e$  is the local, beam-frame electron number density (assumed constant over the spatial scales of interest) and  $r_e = e^2/(4\pi\epsilon_0 m_e c^2)$  is the classical electron radius. In the beam frame, the interaction time is Lorentz-contracted by a factor of  $\gamma$ , and the plasma period is increased by a factor of  $\gamma^{1/2}$  due to electron density dilation. Hence, high-energy conventional cooling systems, both magnetized and unmagnetized, that are designed to cool at  $\gamma \sim 20 - 300$  will likely operate in the short-interaction-time regime. The model presented here assumes  $T_{int} \ll T_{pl}$  and leaves out the Debye screening of the ion potential and the corresponding electron-electron interaction.

As a matter of convenience, we work in a reference frame where the ion remains at rest at the origin of the coordinate system during the interaction time in the cooler. In the beam frame, the dynamics are non-relativistic. The friction force is computed by adding up momentum kicks from binary ion-electron interactions, *subject to the background subtraction procedure* described below. In the limit of a strong magnetic field, to the leading order of canonical perturbation theory (with a small parameter proportional to  $1/B$ ) the electron gyrocenters are confined to cylinders of constant radius equal to the electron's initial impact parameter  $D$ . Therefore, with the Larmor radius equal to zero in the limit of infinitely strong magnetic field, in our model the electron macroparticles move in an effective nonlinear 1D potential:

$$\ddot{z}(t) = -Zr_e c^2 \frac{z}{(z^2 + D^2)^{3/2}}, \quad (3)$$

where  $Z$  is the ion charge number and the  $z$  axis is in the direction of the magnetic field in the solenoid.

The effective potential is a “soft” nonlinear potential, in the sense that the period of oscillations increases with amplitude and both oscillatory and unbounded orbits are possible. (The shortest possible oscillation period  $T_{min} = 2\pi\sqrt{D^3/Zr_e c^2}$  for a given impact parameter  $D$  is realized in the limit of infinitely small amplitude.) Depending on the initial conditions, the electron trajectory can be classified as either unbounded, oscillatory, or technically oscillatory but with a period of oscillation that is larger (possibly, much larger) than the interaction time in the cooler. The net dynamic friction force on the ion is determined by contributions from these three orbit types and, due to the nonlinear nature of the interaction potential, it has to be evaluated numerically.

\* Work supported by the U.S. Department of Energy, Office of Science, Office of Nuclear Physics under Award Number DE-SC0015212.

<sup>†</sup> ilya@radiasoft.net

A subtle point of critical importance in computing the friction force numerically is that, because the dynamic friction force is due to the perturbation of the electron distribution by the ion, it should be computed as the difference between (i) the Coulomb force on the ion from the electron macroparticles moving on the ion-perturbed orbits and (ii) the force from the electron macroparticles with identical initial conditions moving along the orbits not perturbed by the ion. This approach to numerical computation of the dynamic friction force has another important advantage: By virtue of the perturbed and unperturbed trajectories having the same initial conditions, one gains both the cancellation of the bulk background force and the suppression of the diffusive momentum kicks whose origin is in the discrete nature of the electron macroparticle distribution.

## SIMULATION SETUP AND WORKFLOW

For simulations presented here, we worked in the parameter regime of [2], which is broadly relevant to high-energy cooling systems. We assume a locally constant beam-frame electron number density of  $n_e = 4.2 \times 10^{15} \text{ m}^{-3}$ , corresponding to the expectation value of the distance to the nearest (to the ion) electron of  $r_1 \approx 4.9 \times 10^{-6} \text{ m}$ . The beam-frame interaction time in the cooler is taken to be  $T_{int} = 4. \times 10^{-10} \text{ s}$ , or approximately  $0.16 \times T_{pl}$ . We considered two ion species: protons and fully-stripped gold ions ( $Z = 79$ ). For simulations and the parametrized model presented here, we consider the case of the ion velocity parallel to the magnetic field lines, and compute the longitudinal component of the dynamic friction force.

The overall approach is to first compute the dynamic friction force on the ion from the cold electron gas, where, in the reference frame used in our simulations (*i. e.*, centered on the stationary ion), all electron macroparticles have the same initial velocity, equal in magnitude to the ion velocity in the beam frame. Once the friction force is known for the ion interacting with the cold electrons, the dynamic friction force acting on the ion from a gas of warm electrons can be computed by convolution,

$$F_{\parallel}^{(w)}(V_i) = \int_{-\infty}^{\infty} F_{\parallel}^{(c)}(V_i - v_e) f(v_e) dv_e, \quad (4)$$

with superscripts  $w$  and  $c$  indicating the force computed for the ion interacting with the warm and cold electron gas, respectively, and the (arbitrary) distribution density of electrons in the longitudinal velocity space denoted by  $f(v_e)$ . In what follows, we discuss the calculation of the drag force from the cold electron gas and the superscript  $c$  is omitted.

As mentioned, we track pairs of electron macroparticles, the two particles in the same pair having identical initial conditions. One electron in each pair moves in the effective potential of Eq. (3), while the other stays on the unperturbed trajectory. The contribution to the net friction force from each initial condition is then computed from the difference between the momentum kicks imparted to the ion by the two electrons in the same pair over the interaction time.

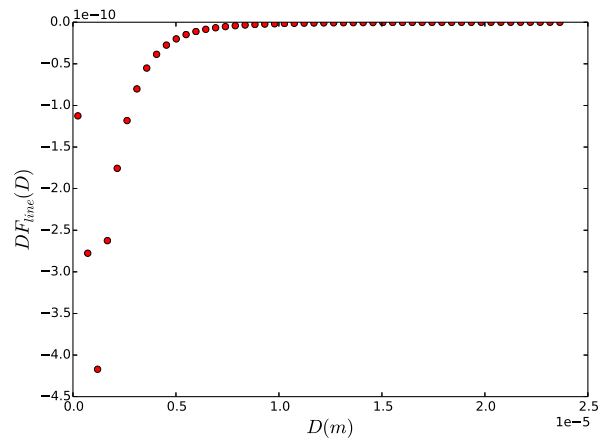


Figure 1: The unnormalized integrand of the r.h.s. of Eq. (5), showing the contribution to the total dynamic friction force from different impact parameters, for a proton with  $V_{\parallel} = 1.5 \times 10^4 \text{ m/s}$  interacting with cold electrons.

We used a second-order, symplectic integrator to generate the results presented in this paper. Taking advantage of the axial symmetry of the configuration under study, we chose the initial conditions along the lines of constant impact parameter  $D$  parallel to the  $z$  axis (for multiple values of  $D$ ). Given the assumption of a constant local density  $n_e$  and our interest in the (ensemble-average) expectation value of the friction force, the initial conditions were spaced uniformly in  $z$ . For a given value of the ion velocity, we first compute the contributions to the total force from all initial conditions with the same impact parameter,  $F_{line}(D)$ , and then integrate over the impact parameters to obtain the total friction force:

$$F_{\parallel}(V_i) = 2\pi n_e \int_0^{\infty} D F_{line}(D) dD. \quad (5)$$

Figure 1 shows the unnormalized integrand of the r.h.s. of Eq. (5) for the case of a proton moving at  $1.5 \times 10^4 \text{ m/s}$ , illustrating two generally valid findings. The first one is that the contributions to the total friction force tend to zero as the impact parameter approaches zero. The second finding is that the large-impact-parameter tail of the integrand falls off approximately exponentially (as seen when plotting the logarithm of the integrand), and so the result for the total friction force is finite even when the integration over the impact parameter is carried out to infinity as the upper limit. (This also allows us to analytically estimate the contributions to the net friction force from impact parameters beyond the largest one that we use in simulations.) Thus, in the model described here, there are *no divergences at either small or large impact parameters* and, therefore, no need to introduce the maximum and minimum cut-off impact parameters and the Coulomb log in order to arrive at a finite value of the friction force.

To compute the longitudinal dynamic friction force as a function of the ion velocity, the procedure outlined in this section is repeated for different values of the ion velocity.

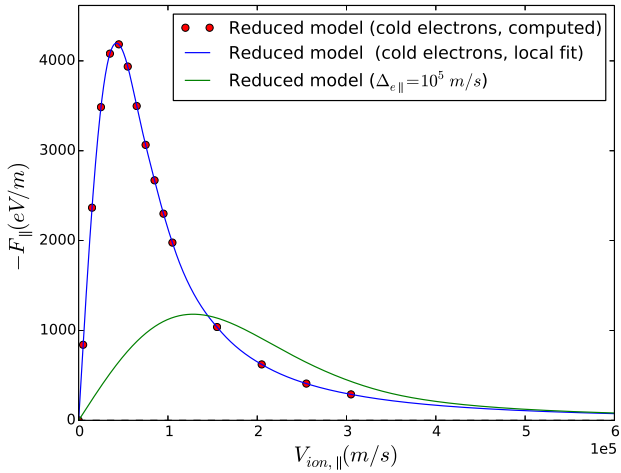


Figure 2: Longitudinal dynamic friction force as a function of the ion velocity, computed from first principles in the limit of infinitely strong B. Gold ion, zero transverse ion velocity component, cold (blue) and warm (green) electrons.

## SIMULATION RESULTS

Figure 2 presents the results of computation of the longitudinal dynamic friction force for the gold ion ( $Z = 79$ ). The beam-frame interaction time  $T_{int} = 4.0 \times 10^{-10} \text{ s}$ . The interpolated cold-electrons result is shown in blue (the red dots are computed values), while the green line shows the result for a warm electron gas, assuming for this example a Maxwellian distribution in beam-frame  $v_{e,\parallel}$  with the rms longitudinal velocity  $\Delta_{e,\parallel} = 1.0 \times 10^5 \text{ m/s}$ . The warm-electrons result was computed via the convolution procedure of Eq. (4). Because convolution with a Gaussian is, in effect, an application of a smoothing filter (a “moving average”), the maximum friction force in a warm electron gas is smaller than the peak dynamic friction force from interaction with cold electrons. For both cold and warm electrons, we find the expected linear dependence of the friction force on the ion velocity at small  $V$ , as well as a  $1/V^2$  dependence at high velocity. The convergence of the “warm” and “cold” results at ion velocities much higher than the rms thermal electron velocity makes sense on qualitative grounds, as well.

Figure 3 shows the computed dynamic friction for protons in a cold gas of strongly magnetized electrons, for three values of the interaction time, namely  $T_{int}$ ,  $0.5 \times T_{int}$ , and  $0.25 \times T_{int}$ . In addition to a linear dependence on the ion velocity at small  $V$ , we find a linear scaling of the friction force in the interaction time. However, the dependence on the interaction time disappears at high ion velocity.

In a study based on a combination of scaling and dimensional analysis and fitting the data, we found the following scaling and asymptotic behavior of the longitudinal friction force computed with our reduced binary interaction model. At low velocity, the friction force is well approximated by

$$F_{\parallel}(V_{\parallel}) \approx -2Zn_e m_e r_e c^2 T_{int} V_{\parallel} \quad (\text{small } V_{\parallel}), \quad (6)$$

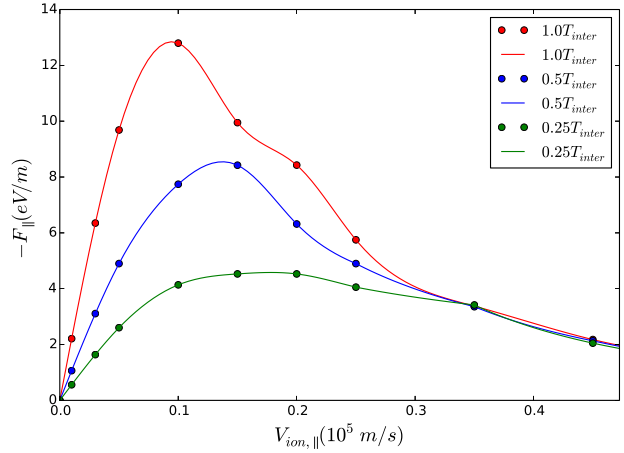


Figure 3: Longitudinal dynamic friction force as a function of the ion velocity, computed from first principles for three different values of the interaction time, in the limit of infinitely strong B. Protons, cold electrons, zero transverse ion velocity component.

with a linear dependence on the ion charge, velocity, and the interaction time. At high ion velocity, the results of the simulations are very well approximated by the expression

$$F_{\parallel}(V_{\parallel}) = -2\pi Z^2 n_e m_e (r_e c^2)^2 / V_{\parallel}^2 \quad (\text{large } V_{\parallel}). \quad (7)$$

that shows a  $Z^2$  dependence on the ion charge number, a  $1/V^2$  dependence on the ion velocity, and no dependence on the interaction time. In addition, the peak friction force scales with the ion charge as  $F_{\parallel}^{max} \propto Z^{4/3}$ .

## PARAMETRIZED MODEL

From our simulation results, we have constructed a simple parametrized model for the longitudinal interaction-time-averaged dynamic friction force on the ion, for the case of strongly-magnetized, longitudinally-cold electrons and short interaction time. In this regime the physical system is described by three independent parameters: the ion charge number  $Z$ , the local electron number density  $n_e$ , and the beam-frame interaction time in the cooler  $T_{int}$ . By construction of our simulation procedure, the friction depends linearly on  $n_e$ . Introducing two auxiliary parameters,

$$A = 2\pi Z^2 n_e m_e (r_e c^2)^2$$

and

$$\sigma \approx (\pi Z r_e c^2 / T_{int})^{1/3},$$

the longitudinal dynamic friction force is given by

$$F_{\parallel}(V) = -\frac{AV}{(\sigma^2 + V^2)^{3/2}}. \quad (8)$$

In addition to correctly capturing the qualitative behavior of  $F_{\parallel}(V)$ , this model reproduces the small- and large-ion velocity asymptotic results of Eqs. (6) and (7). Furthermore,

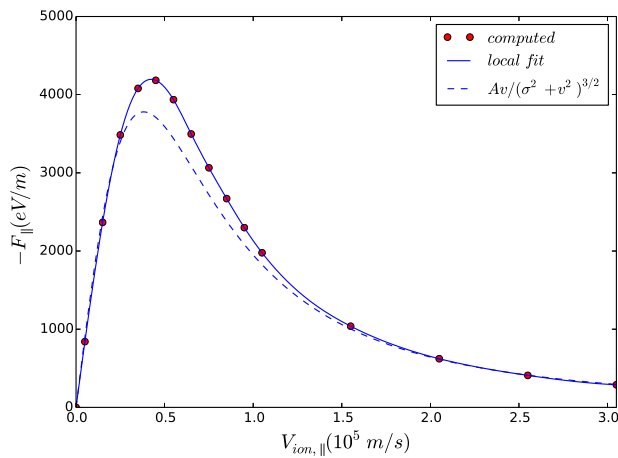


Figure 4: A two-parameter model for the longitudinal dynamic friction force as a function of the ion velocity, Eq. (8), compared with results of first-principles computation in the limit of infinitely strong  $B$ . Gold ion, cold electrons, zero transverse ion velocity component.

the model predicts the scaling of the peak friction force with the ion charge and the interaction time:

$$F_{\parallel}^{max} \propto Z^{4/3} T_{int}^{2/3}, \quad (9)$$

in agreement with empirically found  $Z^{4/3}$  scaling mentioned in the previous section.

Figure 4 illustrates the agreement between the simulation results and our parametrized model for the case of  $Z = 79$  (gold ion). The agreement is generally quite good, although the peak force is underestimated by  $\sim 10 - 15\%$ .

## COMPARISONS WITH ANALYTIC AND SEMI-ANALYTIC MODELS

We compared the results of our first-principles simulations to the predictions of two theoretical models: an analytical expression for the longitudinal friction force in the strong-field limit, due to Derbenev and Skrinsky [1, 3], and the predictions of the semi-analytic model for the magnetized friction force, introduced by Parkhomchuk [4]. In both cases we took the transverse ion velocity to be zero so as to compare the results for the longitudinal magnetized friction force. For the Derbenev and Skrinsky (DS) model, we considered the large-velocity asymptotic limit (the ion velocity is much larger than the longitudinal thermal electron velocity), where their result for the longitudinal friction force simplifies to

$$F_{\parallel}(V_{\parallel}; V_{\perp} = 0) = -\frac{2\pi Z^2 n_e m_e (r_e c^2)^2}{V_{\parallel}^2}, \quad (10)$$

exhibiting a  $Z^2/V^2$  scaling of the friction force, with no dependence on the interaction time and no Coulomb log term. (This is in agreement with [1] and corrects a factor of 2 misprint found in several publications.) For the Parkhomchuk model, we used the definition of the minimum cut-off

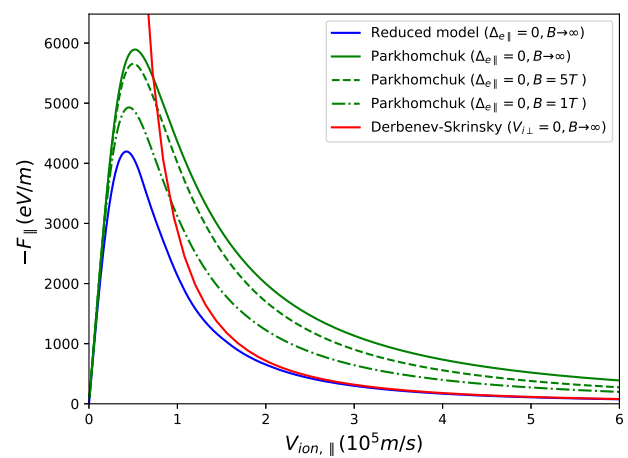


Figure 5: Comparison of the longitudinal dynamic friction force computed from first principles (with the reduced, strong-field model of Eq. (3)) with the predictions of the Parkhomchuk model and the strong-field, high-velocity limit of the Derbenev and Skrinsky model. Results shown are for  $Au^{+79}$  and cold electrons.

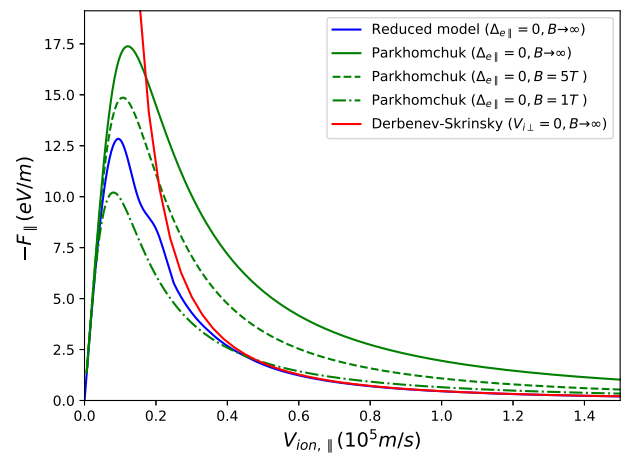


Figure 6: Same as Fig. 5 except the results shown are for protons and cold electrons.

impact parameter  $\rho_{min}$  that enters in the Coulomb log as in BETACOOL [5–7], *i.e.*,  $\rho_{min} = Zr_e c^2 / (V_{ion}^2 + V_{e,eff}^2)$ , taking  $V_{e,eff} = \Delta_{e\parallel}$ , the rms electron thermal velocity. In the Parkhomchuk model, dependence on the magnetic field is via the Larmor gyration radius that enters in the calculation of the Coulomb logarithm, with the infinite- $B$  limit well-defined (non-singular).

For cold electrons, the results of comparison for the gold ion ( $Z=79$ ) and protons are shown in Fig. 5 and Fig. 6. We find an essentially exact agreement with the large-velocity asymptotic of the DS model where the assumptions regarding system parameters are the same as those used in our simulations. It should be noted, however, that while Derbenev and Skrinsky consider a perturbative dielectric response of a plasma, our approach is based on a binary collision model.



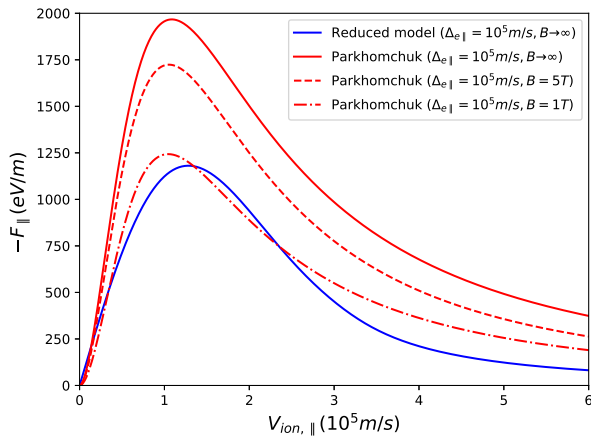


Figure 7: Comparison of the longitudinal dynamic friction force computed from first principles (with the model of Eq. (3)) with the predictions of the Parkhomchuk model with the definition of  $\rho_{min}$  as used in BETACOOl [7]. Results shown are for  $Au^{+79}$  and warm electrons ( $\Delta_{e\parallel} = 1.0 \times 10^5$  m/s).

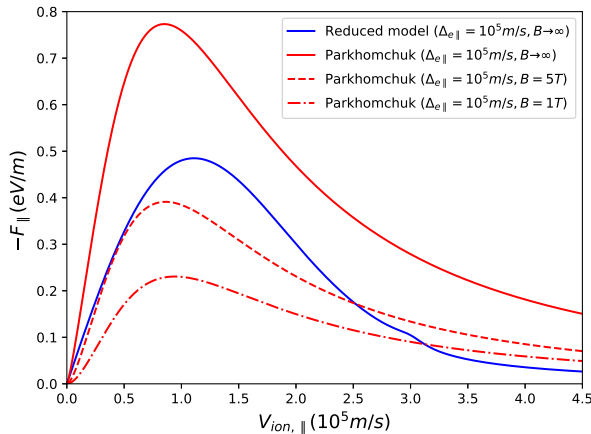


Figure 8: Same as Fig. 7, except the results shown are for protons.

Our longitudinal friction force results are consistently lower, for all ion velocities, than the predictions of the Parkhomchuk model in the strong-field limit. This is also the case for warm electrons, as illustrated in Figs. 7 and 8 for a “representative” choice of the rms electron thermal velocity spread  $\Delta_{e\parallel} = 1.0 \times 10^5$  m/s. This may indicate a possible overestimation of the dynamic friction force in the Parkhomchuk model in this regime. By extrapolation, one may expect to find such overestimation for the finite values of  $B$ , as well.

## DYNAMIC FRICTION FORCE FOR ANTIPROTONS

We applied the approach presented here to compute the longitudinal dynamic friction force acting on an antiproton ( $Z = -1$ ) interacting with a cold, strongly magnetized elec-

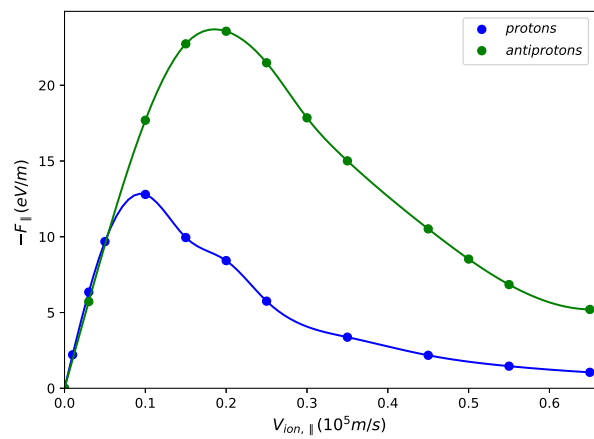


Figure 9: Longitudinal dynamic friction force for protons and antiprotons computed with a reduced ion-electron binary interaction model, assuming a cold, strongly magnetized electron gas.

tron gas, and compare the results to those presented above for protons, keeping system parameters other than the charge number the same. As shown in Fig. 9, our first-principles simulations with the reduced binary collision model yield a significantly stronger friction force for the case of the repulsive ion-electron interaction potential. Qualitatively, this can be traced to the different topology of electron orbits in the repulsive-interaction potential ( $Z < 0$ ) compared to the case of  $Z > 0$ . For  $Z < 0$ , no oscillatory orbits are possible, only unbound orbits and orbits having at most one turn-around point (depending on the  $T_{int}$  and initial conditions). Most of the contribution to the ensemble-averaged net force for  $Z < 0$  comes from strong, small-impact-parameter interactions, yet a finite result for the friction force is obtained when the statistics of the collisions is handled properly. This will be discussed in a separate publication.

## STATISTICAL CONSIDERATIONS

In the work presented here, our objective is to compute the expectation value of the dynamic friction force on a single pass through the cooler. However, estimates of statistical pass-to-pass variations in the momentum kick received by the ion in the cooler are of clear practical interest. Our procedure for computing the friction force makes it possible to estimate, for a given  $T_{int}$ ,  $Z$ , and ion velocity, the volume from which comes (say) 95% of the contribution to the total force on a single pass through the cooler. Assuming a constant  $n_e$ , we then know the number of physical electrons,  $N_{95}$  in this volume. For example, for  $Z = 79$ ,  $V_{ion} = 4.5 \times 10^4$  m/s (near the peak of  $F(V)$ ),  $N_{95}$  is  $\sim 220$ ; while for  $Z = 1$ ,  $V_{ion} = 1.0 \times 10^4$  m/s (near the peak of  $F(V)$  for protons),  $N_{95}$  is  $\sim 20$ . (Clearly, not all of these electrons contribute to the net force equally.) A number as low as 20 indicates a need to look carefully at the statistical properties of diffusive kicks experienced by the ion in traversing the cooler. This will be addressed in greater detail elsewhere.

## REFERENCES

- [1] Ya.S. Derbenev, *Theory of electron cooling*, <https://arxiv.org/abs/1703.09735v2>
- [2] A.V. Fedotov *et al.*, *Phys. Rev. ST Acc. Beams* **9**, 074401 (2006).
- [3] Ya. Derbenev and A. Skrinsky, *Part. Accel.* **8**, 235, 1978.
- [4] V. Parkhomchuk, *Nucl. Instrum. Methods Phys. Res., Sect. A* **441**, 9, 2000.
- [5] A.O. Sidorin *et al.*, *Nucl. Instrum. Methods Phys. Res., Sect. A* **558**, 325, 2006.
- [6] A. O. Sidorin and A. V. Smirnov, *ICFA Beam Dynamics Newsletter* **65**, 127, 2014.
- [7] I. Meshkov, A. Sidorin, A.V. Smirnov, G.V. Trubnikov, and A. Fedotov, *BETACOOOL Physics Guide*, <http://lepta.jinr.ru/betacool>